21

Moth-Like Chemo-Source Localization and Classification on an Indoor Autonomous Robot

Lucas L. López et al.*
SPECS, Technology Department, Universitat Pompeu Fabra and ICREA
Spain

1. Introduction

Olfaction is a crucial sense for many living organisms. Many animals, especially insects, rely heavily on the olfactory sense for encoding and processing different chemical cues in order to perform several tasks such as foraging, predator avoidance, mate finding, communication etc.(22). Yet, olfaction has not been as widely studied as vision or the auditory system in insects. At the same time, robotic platforms capable of searching, locating and classifying odor sources in wind turbulence and in the presence of complex odors have diverse applications ranging from environmental monitoring (21), detection of explosives and other hazardous substances (19), land mine detection (2) to human search and rescue operations. The main challenge thereby is the stable and fast coding and decoding of odors and the localization of the sources (17).

In our own recent work, we have proposed an insect-like mapless navigation mechanism which integrates surge-and-cast chemo search, path integration, wind detection and visual landmark navigation on an indoor mobile robot (28). Also, we have proposed a model based on insect navigation that is capable of navigating in highly dynamic environments and our model was compared directly to ant navigational data, with strikingly similar navigational behaviors (26). The problem of ambiguous information, particularly in the navigational context, is also addressed in our recent work (27). Beyond that, we have contributed significantly to modeling insect navigation and designing robotic systems such as: a model of the locust Lobula Giant Movement Detector (LGMD) tested on a high speed robot (29), moth-like odor localization for robots (30), control of an unmanned aerial vehicle using a neuronal model of a fly-locust brain (31; 32), moth-like optomotor anemotactic chemical search for robots (33), and a blimp flight control using a biologically inspired flight control system (34).

Despite these advances, several biological systems with relatively simple nervous systems solve the odor localization and classification problem much more efficiently than their artificial counterparts: bees use odor to localize nests, ants use pheromone trails to organize foraging in swarms, lobsters use odor to locate food, the *Escherichia* bacteria use odors to locate nutrients, male moths use olfaction to locate female mates etc. The odor localization

*Vasiliki Vouloutsi, Alex Escuredo Chimeno, Encarni Marcos, Sergi Bermúdez i Badia, Zenon Mathews, Paul F.M.J. Verschure (*SPECS, Technology Department, Universitat Pompeu Fabra and ICREA, Barcelona*), Andrey Ziyatdinov, Alexandre Perera i Lluna (*Departament d'Enginyeria de Sistemes, Automàtica i Informatica Industrial, Universitat Politècnica de Catalunya and CIBER-BBN in Bioengineering, Biomedicine and Nanomaterials, Barcelona*)

task can be divided into three general steps (9): 1) search and identification of the chemical compounds of interest in the given environment, 2) tracking the odor until its source guided by chemical and all other available sensory modalities, 3) and finally identifying the source (either by vision or e.g. by olfaction using the odor concentration pattern that is acquired in a specific restricted area). However, in real world applications, locating the source of a chemical plume and classifying the chemical are difficult tasks due to the fact that the plume dispersion dynamics vary heavily depending on the medium. The chemical volatiles in the atmosphere are mainly transported by airflow and the interaction of the airflow with other surfaces and sources of thermal gradients produce turbulence. This chemical dispersion is best described by the Reynolds number. At low Reynolds values, there is a monotonic decrease of the chemical concentration, however at medium and high values turbulence dominates. Thus different search and classification strategies should be employed in these different environments (9).

The rich availability of insect odor coding and localization studies have inspired several biologically inspired robots that perform odor localization and classification: underwater robots (6), ground robots (14) and even flying robots (2). Nevertheless, stable odor source localization and classification using fully autonomous robots have not yet been demonstrated. We here propose a moth based model of odor localization and classification and its implementation on an embedded autonomous robot in a controlled indoor wind tunnel setup. For odor coding and localization at high Reynolds values where turbulence prevails, we use a model of odor source localization and odor classification mechanism suggested to be employed by the male moth. Our embedded robot is controlled using a neural network model of the moth olfactory pathway implemented using the large scale neuronal simulator IQR (4), that runs on board the embedded robot. Our results show the first steps towards stable odor localization and classification using a completely autonomous robot that is controlled by a neuronal model of the moth olfactory system.

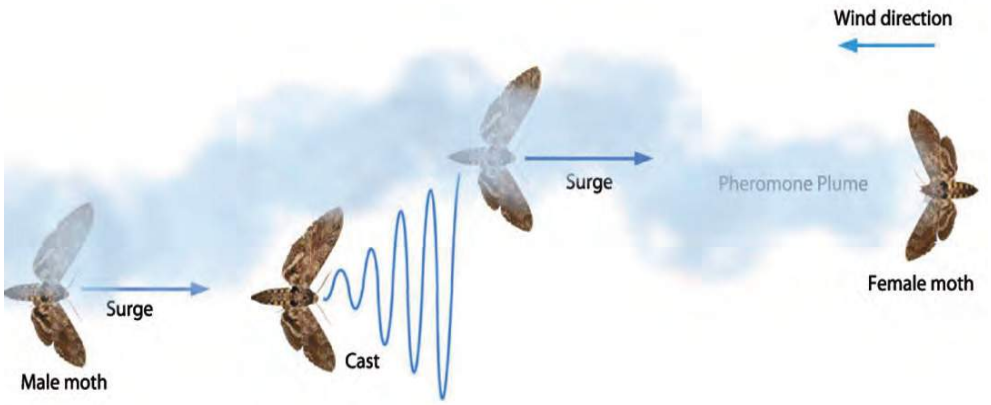

Fig. 1. Illustration of the cast and surge male moth behaviour and the female pheromone plume.

2. Methods

Insects in general and moths in particular are able to locate a source of odor and distinguish it from different other sources. Our model of olfaction is based on the male moth behavior and

physiology. In this section we explain our olfactory model proposed for solving the problem of odor localization and classification, the robot platform and the experimental set-up used to assess its performance.

2.1 Cast & Surge

The male moth has been widely studied because of its unique ability to find mates by detecting low pheromone concentrations over large spatial scales. When the female moth releases a pheromone blend, this blend flows downwind creating a specific plume shape. When the male moth detects the pheromone plume, it starts flying upwind, tracing the pheromone molecules in the plume, a stereotypical behavior called *surge*. However, as the structure of the plume is quite complex and unpredictable, the male moth looses track of the pheromone plume often during the surge behavior. For this reason, the male moths have developed a behavior that allows them to re-discover the pheromone plume again. This behavior is called *cast* and is a zigzag movement orthogonal to the wind direction (17) (see Figure 1). The casting frequency increases and the speed decreases when close to the source (10).

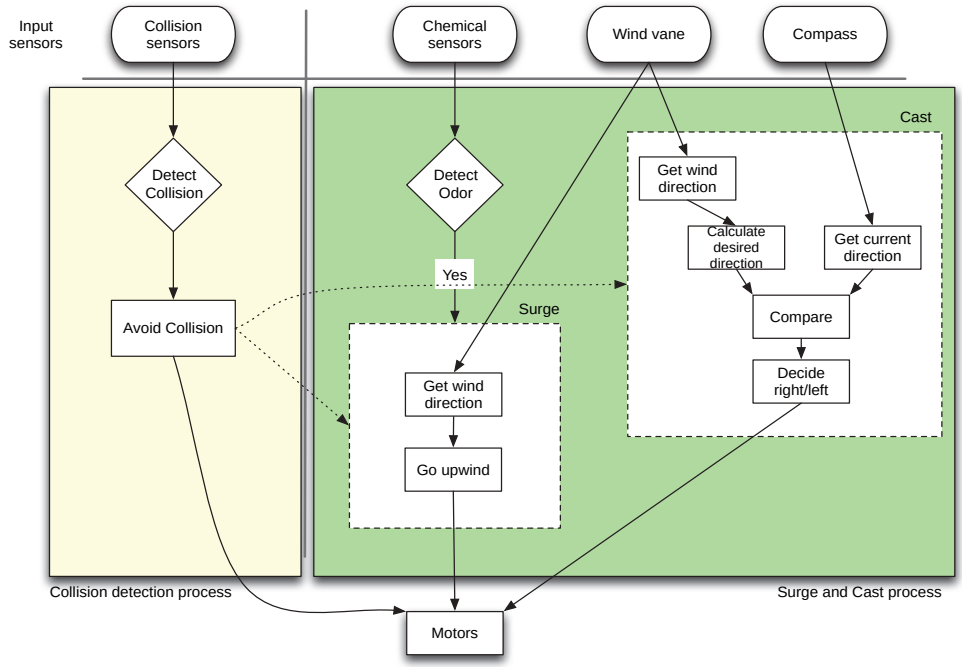

Fig. 2. Scheme of the system implemented for the cast and surge behaviour. It consists of two processes: *collision detection* and *surge and cast*. Dashed arrows indicate inhibitory influences.

Our model of odor localization is based on this cast and surge behavior of the male moth. The architecture of the system consists of two process that run in parallel: *collision detection* and *surge and cast* (see figure 2). The *collision detection process* has higher priority and inhibits dashed arrow in figure 2) the *surge and cast* process. The *surge and cast* process performs the localization of the odor source. When the chemical sensors detect an odor the robot performs

a surge behaviour, and otherwise a cast is executed. The processes are implemented using leaky Integrate and Fire (IF) and leaky Linear Threshold (LT) neurons (16; 20).

2.2 Classification

While being able to locate an odor source, the male moths are also able to distinguish among similar stimuli and to classify different concentrations of the same chemical into the same stimulus category. The olfactory pathway is composed of Olfactory Receptor Neurons (ORNs) in the antenna, the Antennal Lobe (AL) and the Mushroom Body (MB) (7) (see Figure 3). ORNs are distributed over the antenna and respond to different chemical stimulus present in the air. ORNs expressing similar receptors usually converge onto a single glomerulus in the AL. The number of glomeruli is then closely related to the number of ORN classes. This convergence of ORNs into the same glomeruli makes the AL capable of dealing with noisy conditions and dynamic inputs (11).

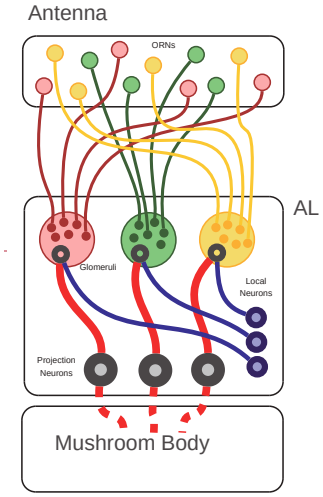

Fig. 3. Functional representation of a generic AL. ORNs belonging to the same class converge onto the same glomerulus. LNs interconnect PNs which is connected to higher brain areas such as the MB.

Two different types of neurons receive input from ORNs: Projection Neurons (PNs) and Local Neurons (LNs). PNs integrate the activity from the glomeruli and forward it to the MB, which is known to be involved in the learning and memory of odors (24). LNs laterally interconnect PNs and modify their activity by means of inhibition.

We use a modified implementation of the model proposed by (15). The original model uses a group of Integrate-and-Fire neurons as Projection Neurons, which receive constant excitation, interconnected with two groups of Local Neurons. These LNs are connected in such a way that when a specific pattern is presented to the network, concrete PNs will fire synchronously. When the pattern disappears from the input, the neurons get desynchronized. These synchronization and desynchronization processes can be explained with two concepts: a combination of transient resetting and the probability of failure of synapses between the Local Neurons and the Projection Neurons. Transient Resetting has been theoretically described by (13) as a way to enhance the spike timing precision on a group of neurons, caused by a loss of initial conditions. In the presented model the current pulse coming from the LNs

to the PNs allow the latter to turn from their state to their resting potential, which makes the next spike to happen simultaneously. The presence of noise in the connection between LNs and PNs has an essential role in the network equilibrium. LNs interconnect PNs in two different ways: via fast ($GABA_A$ type) and slow ($GABA_B$ type) inhibition. The failure of these synapses has been set to 50%. The key concept is that when fast inhibition is not greatly affected by the failure of a connection and is still able to produce the transient resetting, the slow inhibition is much more sensitive and has the opposite effect, generating noise in the inter-neuron spike timing.

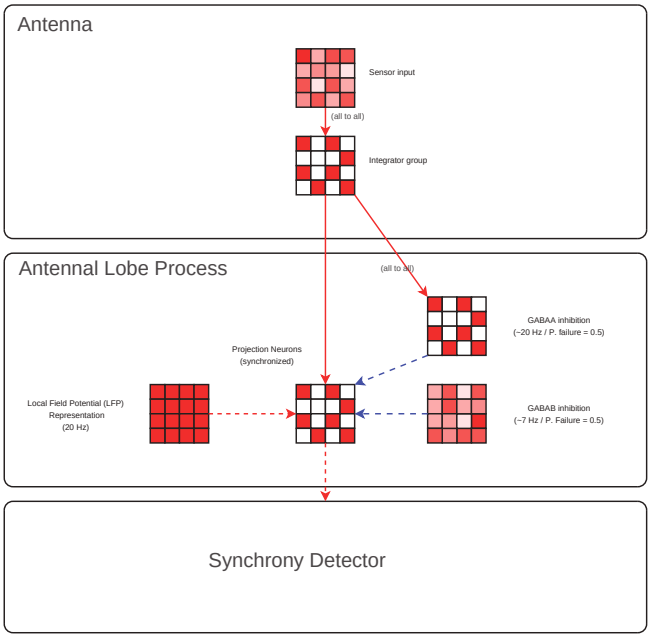

Fig. 4. Scheme of the system implemented for the odor classification. Red arrows indicate excitatory connections and blue arrows indicate inhibitory connections.

This model proposed by(15) was designed to receive only binary input patterns. The model needed to be adapted for real world conditions where the sensory input is analog. Based on the modification proposed by (12), we use a group of neurons that process the input from the sensors to extract a binary pattern that is later fed into the AL model. The numeric parameters from the original model has been respected as much as possible in order to obtain similar results. Fast $GABA_A$ inhibitions oscillate around $20Hz$, while $GABA_B$ frequency is around $8Hz$. The interconnection topology between PNs and LNs also respect the original setup: if the PN responds to the odor stimuli, it has $GABA_A$ and $GABA_B$ inhibitory interconnections, whereas if it does not respond to the odor stimuli, it has only $GABA_B$ inhibitory interconnections. Figure 4 shows a scheme of the system.

2.3 The robot

2.3.1 Robotic platform

The autonomous robot used for the experiments is composed of two parts, a mobile platform developed in SPECS at UPF and an embedded computer assembled at UPC, both designed in

the scope of the Bio-ICT European project NEUROChem (Figure 5). The basic requirements applied to the robot include full autonomy, demonstration capabilities and full-functioning interface with chemical and other navigation sensors.

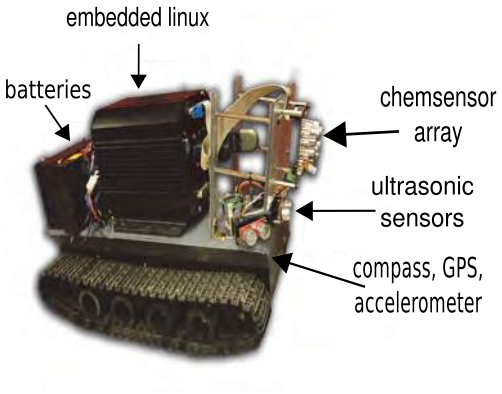

Fig. 5. Image of the autonomous robotic platform.

The mobile platform is driven by motors acting on two caterpillar tracks on both sides, and holds different sensory electronics for robot navigation such as ultra sonic distance sensors, compass, GPS and accelerometer. The mobile base is interconnected with the embedded platform either via Bluetooth or by the USB cable.
The embedded computer performs functions of a host platform targeted to high-performance sensor data acquisition as presented on Figure 6. The use of the embedded technology for the moth robot is motivated by several factors. The embedded computer runs a custom GNU/Linux image to control the complete robotic system with the aid of the standard desktop solutions. Moreover, the computational resources are needed for the real-time acquisition, processing and visualization of the sensory data coming from the real world, and especially for capturing the chemical stimuli. Moreover, the execution of the biomimetic models of the antennal lobe and the mushroom body requires a solid software framework hosted on the computer.
The success of the odor localization task highly depends on the instrumentation capabilities of the robot for odor sensing, that is traditionally based on an array of broadly-selective gas sensors (18). The robot design allows to host three types of the gas sensor arrays providing specific hardware interfaces, scanning electronic boards and signal processing software.
The main large-scale array contains 64K polymeric sensors (16 modules of 64×64 sensing elements each) and around 8 of sensor types (1). The critical parameter is the acquisition speed of a sensor, which is determined by dynamics of the chemical reactions in sensor device and limited by transient constants of the read-out electronic circuit (proportional to parasitic capacitances). The preliminary experiments (1) showed the sampling rate of $\approx 293\ \mu_s$ for a sensor. Due to the modular structure of both the sensor array and the acquisition boards, the acquisition speed for the complete number of sensors (64 K) expected to be close to $1.8\ s$. That seems reasonable to perform the real-time robot experiments.
The preliminary results presented in this work are obtained with the second sensor array, as the main polymeric array is still in the development phase. The current array is composed of 16 MOX sensors of 4 Figaro (Figaro Engineering Inc) types (TGS 2442, TGS 2612, TGS 2610 and TGS 2600). The third array supported by the platform, referred as to virtual sensor array (25),

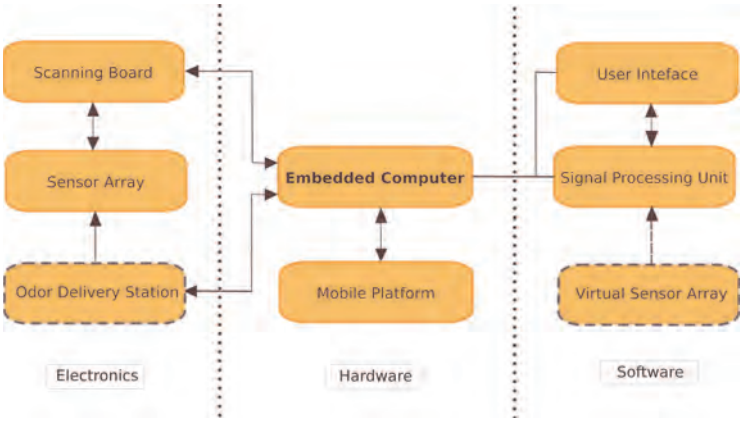

Fig. 6. Architecture of the robotic platform.

represents a software abstraction of sensor signals used during testing the insect olfactory models.

2.3.2 PC104-based embedded computer

The architecture of the embedded computer is based on the well-established PC104 standard that was originally proposed as an extension of the IEEE-P996 standard (Standard for Compact Embedded - PC Modules). PC104 systems are typically industrial rugged embedded applications where reliable data acquisition is needed in an extreme environment.
The key features of the PC104 bus in comparison with the regular PC bus (IEEE P996) include: compact form-factor (reduced from from 3.8 to 3.6 inches), the unique self-stacking bus, the pin-and-socket connectors and lower power consumption.
Figure 7 shows the structure of the embedded computer and its PC104 component boards: CPU board PCM-3372F-S0A1E (Advantech), data acquisition board PC104-DAS16Jr/16 (Measurement Computing), Power Supply Unit HESC104 and Battery Pack BAT-NiMh45 (Tri-m Systems).
The main CPU board is a single-board computer (no division into the mother-board and other daughter-boards, instead, the design is centered on a single board), of which the specification characteristics make it close to a small laptop computer. The board has Intel Ultra-Low Voltage fanless VIA Eden V4 1.0 GHz processor, 1GB RAM of DDR2 standard at 533 MHz, and the system chipset VIA CX700 with 64MB VRAM.
The I/O periphery consists of two serial ports, six USB 2.0, keyboard/mouse slots, audio and 8-bit GPIO ports, 10/100 Mbps Ethernet interface, and a slot for flash type I card.
The data acquisition unit is a 16-channel board with ADC 16 channels with 16 bit resolution. Such configuration of the card allows that the data acquisition from the sensor array from 16 channels in parallel, that in turn speeds up the processing by a factor of 16. The maximum acquisition rate of 100KHz is more than enough to read the signals from the sensor array, as the maximum read-out speed on the sensor scanning electronics is not greater than 4KHz. The input range in the unipolar mode is set to [0; 5]V and [0; 10]V, for polymeric and MOX sensor array respectively. The DMA mode support is implemented to reduce the CPU overhead during the data read-out.

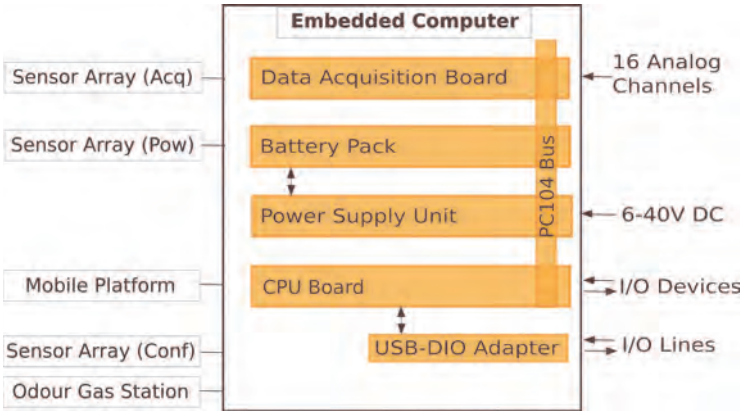

Fig. 7. The PC104-based embedded computer.

The power supply unit is a DC-DC converter with a wide range of input voltage from 6V to 40V DC and the output power if 60W. The UPS mode is supported with board configuration stored in the EEProm memory.
The power consumption of the embedded computer in the complete configuration is typically 9W (maximum of 15.5W). The polymeric sensor array with 64K elements requires from 4W to 10W. Given the maximum power consumption 25.5W, the selected battery pack with capacity 500 mA per hour will guaranty an autonomous operation around 1.1 hour.

2.3.3 Software layer

The models for odor localization and classification have been implemented using IQR (see figure 8), a multilevel neuronal simulation environment that provides a tool for graphically designing large-scale real-time neuronal models (3). It is designed to visualize and analyze data on-line and interfacing to external devices like robots are possible thanks to its modular structure. IQR applications thus acquire data from the robot sensors, process them using the above described models of odor source localization and classification and finally sends motor commands to the robot in real-time.

2.4 Experimental set-up

The experimental scenario is a controlled indoor environment. The robot is tested in two main tasks: (1) odor localization; (2) odor classification. The scenario uses a wind tunnel that creates an odor plume where the robot can freely move. To track the trajectory of the robot and compute its heading direction inside the wind tunnel we use an overhead tracking camera. The chemical compounds used to test the odor classification are ethanol and acetone diluted in distilled water. An ultrasonic source is used to disperse the chemical compounds and generate a rapidly evaporating mist.

2.4.1 The wind tunnel

The conducted experiments took place in a wind tunnel which was located at the SPECS lab in Barcelona, Spain. The wind tunnel is made of a wooden skeleton and is covered with a transparent polyethylene sheet of low density. It consists of two main modules: the first one is the main tunnel - a controlled space where the robot is placed and can freely move. The second part is where the air-flow is generated, using four exhaust ventilators to create

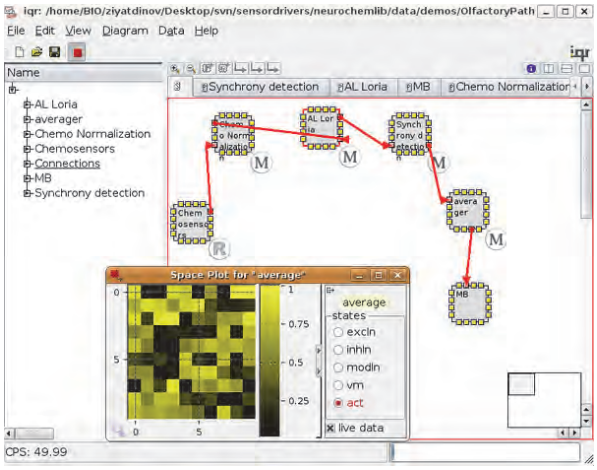

Fig. 8. The iqr simulation environment running the olfactory system of the insect. Space plot shows the neuronal activity of a prototypical neuronal group.

negative pressure. The plume that is created moves across the whole wind tunnel from the point of the odor source to the ventilators where the air is extracted out of the experiment room. Each ventilator is a 4.4KW centrifugal fan and the flow velocity within the wind tunnel is up to 1.0 m s^{-1}. The wind tunnel has to be large enough for the robot, and therefore is 3 meters wide, 4 meters long and 54 centimeters high. For the odor localization experiment, the starting point of the robot was set in front of the fans which is the outlet of the wind tunnel and the odor source was placed in the upwind end of the wind tunnel (see figure 9).
As for the classification experiment we needed to have more stable conditions we placed the robot in the mid spatial position inside the wind tunnel. The odor was spread through the tunnel during five minutes before running the experiment. Additionally, the robot remained in the initial position during the whole the experiment. These two restrictions kept the sensory input as stable as possible. This task was tested with two different odors composed of ethanol (20%) or acetone (20%).

2.4.2 Vision based tracking system (AnTS)

To track the robot's trajectory, a monochrome camera is placed 3 meters above the testing arena. An IR filter is added to the camera to allow the system to track the robot independently of the light conditions. AnTS, a vision based tracking system is used to identify the three points created by the robot's IR LEDs. It computes the robot's orientation and absolute position inside the wind tunnel.

3. Results

Two main experiments were conducted to test the odor classification and the casting behavior of the robot. The latter was performed to assess the odor localization strategy implemented on the robot and the former to assess the robot's ability to classify chemical compounds. Both experiments were conducted in the wind tunnel.

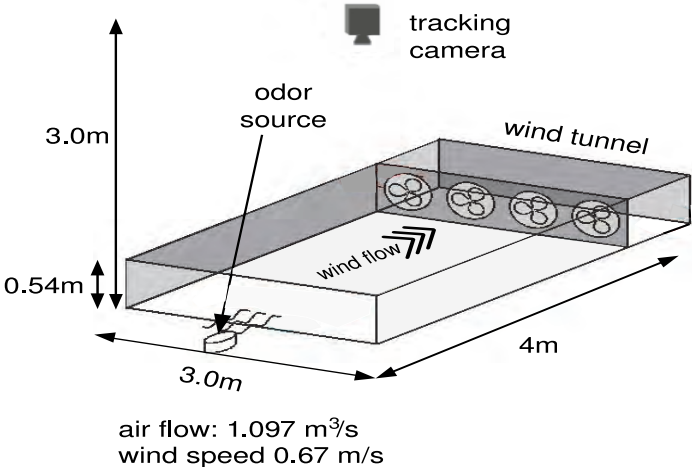

Fig. 9. Layout of the wind tunnel including the position of the camera of tracking system. Red arrows show the wind flow direction from the odor source towards the end where four fans extract the flow out of the tunnel.

3.0.3 Chemical plume in the wind tunnel

First we performed a guided tour of the robot through the wind tunnel to log the sensory data together with the robot position in order to assess the general pattern of chemosensor readings. Figure 10 shows the summed response of the chemosensors for the different robot positions inside the wind tunnel with two chemical sources (Ethanol 1% and Acetone 1%), showing the plume pattern inside the tunnel.

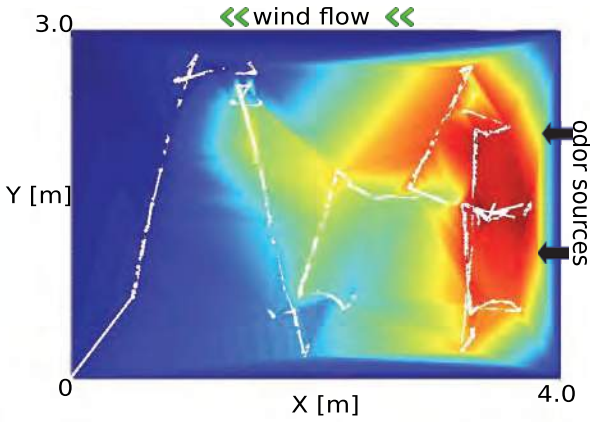

Fig. 10. Chemo sensor readings sampled at different points (white dots) by the robot inside the wind tunnel. The overall plume intensity is captured by the heat plot using the summed input of all 16 chemical sensors.

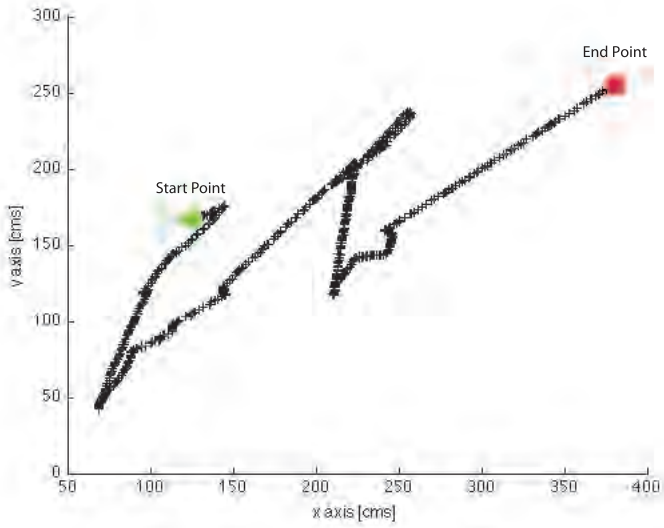

Fig. 11. Robot position plot while casting. The robot is placed in the downwind end of the wind tunnel, in front of the ventilators facing upwind with the chemosensors. The initial point of the robot is marked in the green spot and the end point in red.

3.0.4 Chemosearch

We first discuss the casting behavior of the robot. The robot was placed in the downwind end of the wind tunnel facing upwind. As mentioned above, the moth olfactory model performs a surge when a chemical plume is detected by the sensors and a cast when the plume is lost. In the first experiment we tested the casting model to investigate the explorative behavior with no chemical compounds present. To calculate the robot's trajectory, we performed an offline analysis of the collected robot position data. Figure 11 shows the trajectory of the robot while casting. Our results show a correct crosswind casting movement as no chemicals are detected. However, the casting does not cover the wind tunnel breadth, the main reason being the restricted maneuverability of the current robotic platform. Nevertheless, this preliminary result is promising since the casting model works as expected, reproducing a crosswind cast.

3.0.5 Classification

The results in classification show a successful synchronization of the foreground neurons corresponding to the pattern in both experiments. The Projection Neuron (PN) output is fed to a synchrony detector group implemented in iqr. The plume testing experiments were conducted for a variety of concentration ranges from 1% to 20%.

4. Conclusions and discussion

We have demonstrated the implementation of an autonomous embedded robot that performs moth-like chemosearch and classification strategies. Our models are implemented using the IQR large-scale neuronal simulator and runs on-board the embedded computer. The robot is capable of performing autonomous casts inside the wind tunnel and of classifying two different odors. Nevertheless, we observe that the maneuverability of the robot is restricted:

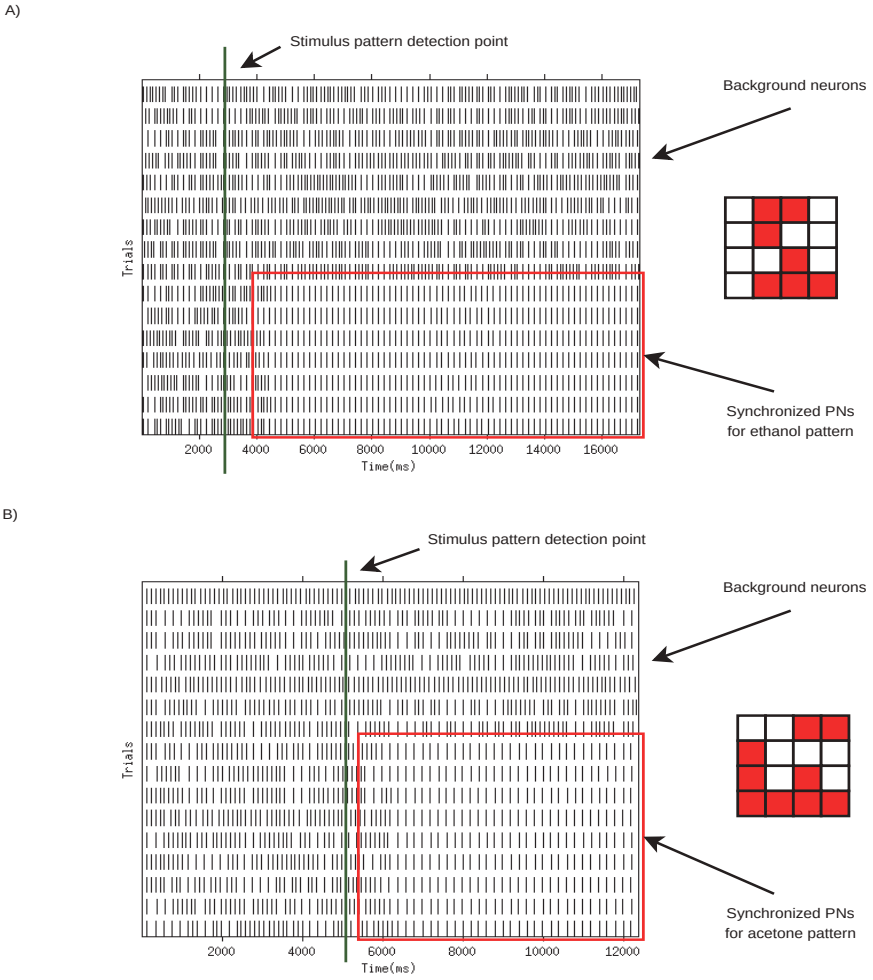

Fig. 12. Raster-plot of the two experiments for the 16 input neurons. The neurons have been grouped into foreground and background neurons of the corresponding patter. The first period corresponds to the time the integrator needs to recognize the pattern (5 and 3 seconds respectively). Once the pattern was input to the network (green line), it would make the corresponding neurons to spike synchronously in about 1 second. The synchrony detector effectively shows the pattern at the output when the specific neurons were synchronized with respect to the background neurons.

the motors are too fast to perform controlled surge and cast. We currently are building a new robotic platform that achieves lesser speed and has a lesser turning radius. The classification results can be considered as a proof of concept for the possibility to classify odors with the antennal Lobe model proposed in (15) and adapted in (12). However, the capability of this model to actually distinguish mixtures of components with real sensor signals and with dynamic input (i.e. a moving robot), or to act in the presence of a distractor in the

environment are not yet clear. Further work is intended as extensions of this model with Temporal Population Coding (TPC) strategies, which has been suggested and is consistent with both vertebrate and invertebrate physiology (5; 8; 23).

5. Acknowledgments

The research leading to these results has received funding from the European Community's Seventh Framework Programme (FP7/2007-2013) under grant agreement no. 216916 for the NEUROCHEM project.

6. References

[1] Beccherelli, R., Zampetti, E., Pantalei, S., Bernabei, M. & Persaud, K. C. (2009). Very large chemical sensor array for mimicking biological olfaction, *OLFACTION AND ELECTRONIC NOSE: Proceedings of the 13th International Symposium on Olfaction and Electronic Nose* 1137(1): 155–158.

[2] BermÃždez, S., Bernardet, U., Guanella, A., Pyk, P. & Verschure, P. F. (2007). A biologically based chemo-sensing uav for humanitarian demining, *International Journal of Advanced Robotic Systems* 4(2): 187–198.

[3] Bernardet, U., Blanchard, M. J. & Verschure, P. F. M. J. (2002a). Iqr: a distributed system for real-time real-world neuronal simulation, *Neurocomputing* 44-46: 1043–1048.

[4] Bernardet, U., Blanchard, M. & Verschure, P. F. M. J. (2002b). Iqr: a distributed system for real-time real-world neuronal simulation, *Neurocomputing* 44-46: 1043–1048.

[5] Carlsson, M. A., KnÃijsel, P. & P. F. M. J. Verschure, B. S. H. (2005). Spatio-temporal ca2+ dynamics of moth olfactory projection neurones., *Eur J Neurosci* pp. 647–657.

[6] Grasso, F. W., Consi, T. R., Mountain, D. C. & Atema, J. (2000). Biomimetic robot lobster performs chemo-orientation in turbulence using a pair of spatially separated sensors: Progress and challenges, *Robotics and Autonomous Systems* 30(1-2): 115–131.

[7] Hansson, B. S. (2002). A bugâĂŹs smellâĂŞresearch into insect olfaction., *Trends Neurosci* pp. 270–224.

[8] Knüsel, P., Carlsson, M. A., Hansson, B. S., Pearce, T. C. & Verschure, P. F. M. J. (2007). Time and space are complementary encoding dimensions in the moth antennal lobe, *Network (Bristol, England)* 18(1): 35–62.

[9] Kowaldo, G. & Russell, R. A. (2008a). Robot odor localization: A taxonomy and survey, *The International Journal of Robotics Research* 27(8): 869–894.

[10] Kowaldo, G. & Russell, R. A. (2008b). Robot odor localization: a taxonomy survey, *The International Journal of Robotics Research* 27(8): 869–894.

[11] Laurent, G. (1999). A systems perspective on early olfactory coding., *Science* pp. 723–728.

[12] Lechón, M., Martinez, D., Verschure, P. F. M. J. & i Badia, S. B. (2010). The role of neural synchrony and rate in high-dimensional input systems. the antennal lobe: a case study., *International Joint Conference on Neural Networks*.

[13] Li, C., Chen, L. & Aihara1, K. (2006). Transient resetting: a novel mechanism for synchrony and its biological examples., *PLoS Computational Biology* .

[14] Liu, Z. & Lu, T. (2008). Odor source localization in complicated indoor environments, *2008 10th International Conference on Control, Automation, Robotics and Vision* pp. 371–377.

[15] Martinez, D. & Montejo, N. (2008). A model of stimulus-specific neural assemblies in the insect antennal lobe, *PLoS Computational Biology* .

[16] McCulloch, W. & Pitts, W. (1943). A logical calculus of ideas immanent in nervous activity, *Bulletin of Mathematical Biophysics* 5: 115–113.

[17] Pearce, T., Chong, K., Verschure, P. F., i Badia, S. B., Chanie, M. C. F. & Hansson, B. (2004). Chemotactic search in complex environments: From insects to real-world applications, *Electronic Noses & Sensors for the Detection of Explosives* (159): 181–207.

[18] Persaud, K. & Dodd, G. (1982). Analysis of discrimination mechanisms in the mammalian olfactory system using a model nose., *Nature* 299(5881): 352–355.

[19] Rachkov, M. Y., Marques, L. & de Almeida, A. (2005). Multisensor demining robot, *Autonomous Robots* 18(3): 275–291.

[20] Stein, R. (1967). Some models of neuronal variability, *JBiophys* 7: 37–68.

[21] Trincavelli, M., Reggente, M., S.Coradeschi, Loutfi, A., Ishida, H. & Lilienthal, A. J. (2008). Towards environmental monitoring with mobile robots, *Proceedings of the 2008 IEEE/RSJ International Conference on Intelligent Robots and Systems* pp. 2210–2215.

[22] von Frisch, K. (1974). Decoding the language of the bee, *Science (New York, N.Y.)* 185(4152): 663–668.

[23] Wyss, R., KÃűnig, P. & Verschure, P. F. M. J. (2003). Invariant representations of visual patterns in a temporal population code., *Proc Natl Acad Sci U S A* pp. 324–329.

[24] Zars, T., Fischer, M., Schulz, R. & Heisenberg, M. (2000). Localization of a short-term memory in drosophila, *Science* 288(5466): 672–675.

[25] Ziyatdinov, A., Fernandez-Diaz, E., Chaudry, A., Marco, S., Persaud, K. & Perera, A. (2011). A large scale virtual gas sensor array, *International Symposium on Olfaction and Electronic Nose (ISOEN 2011)* .

[26] Z.Mathews and Sergi Bermúdez i Badia and Paul F.M.J. Verschure, *An Insect-Based Method for Learning Landmark Reliability Using Expectation Reinforcement in Dynamic Environments* IEEE International Conference on Robotics and Automation (ICRA2010)

[27] Zenon Mathews and Sergi Bermúdez i Badia and Paul F. M. J. Verschure, *Action-Planning and Execution from Multimodal Cues: An Integrated Model for Artificial Autonomous Systems* Springer-Verlag, Studies in Computational Intelligence 2010

[28] Zenon Mathews and Miguel Lechón and Jose Maria Blanco Calvo and Anant Dhir and Armin Duff and Sergi BermÃždez i Badia and Paul F. M. J. Verschure, *Insect-Like Mapless Navigation Based on Head Direction Cells and Contextual Learning Using Chemo-Visual Sensors* The 2009 IEEE/RSJ International Conference on Intelligent RObots and Systems (IROS2009), 2009

[29] Sergi Bermúdez i Badia and Ulysses Bernardet and Paul F.M.J. Verschure , *Non-Linear Neuronal Responses as an Emergent Property of Afferent Networks: A Case Study of the Locust Lobula Giant Movement Detector*. PLoS Computational Biology. 2010, 6(3)

[30] Sergi Bermúdez i Badia and Paul F. M. J. Verschure, *Learning from the Moth: A Comparative Study of Robot-Based Odor Source Localization Strategies*, 13th International Symposium on Olfaction and Electronic Nose 2009.

[31] Sergi Bermúdez i Badia and Paul F. M. J. Verschure, *Humanitarian Demining Using an Insect Based Chemical Unmanned Aerial Vehicle*, Humanitarian Demining 2008

[32] Sergi Bermúdez i Badia and Pawel Pyk and Paul F. M. J. Verschure, *A fly-locust based neuronal control system applied to an unmanned aerial vehicle: the invertebrate neuronal principles for course stabilization,altitude control and collision avoidance*, The International Journal of Robotics Research. 2007, 26(7), 759-772.

[33] Pawel Pyk, Sergi Bermúdez i Badia, Ulysses Bernardet, Philipp Knüsel, Mikael Carlsson, Jing Gu, Eric Chanie, Bill S. Hansson, Tim C. Pearce, Paul F. M. J. Verschure , *An artificial moth: Chemical source localization using a robot based neuronal model of moth optomotor anemotactic search*, Autonomous Robots 2006, 20(3), 197-213.

[34] Sergi Bermúdez i Badia, Pawel Pyk, Paul F. M. J. Verschure, *A Biologically Inspired Flight Control System for a Blimp-based UAV*, ICRA 2005. 3053-3059.